

# Mechanisms of Noise-Induced Improvement in Light-Intensity Encoding in *Hermisenda* Photoreceptor Network

Christopher R. Butson and Gregory A. Clark

*J Neurophysiol* 99:155-165, 2008. First published 14 November 2007; doi:10.1152/jn.01250.2006

---

## You might find this additional info useful...

---

This article cites 35 articles, 7 of which can be accessed free at:

<http://jn.physiology.org/content/99/1/155.full.html#ref-list-1>

Updated information and services including high resolution figures, can be found at:

<http://jn.physiology.org/content/99/1/155.full.html>

Additional material and information about *Journal of Neurophysiology* can be found at:

<http://www.the-aps.org/publications/jn>

---

This information is current as of March 1, 2011.

# Mechanisms of Noise-Induced Improvement in Light-Intensity Encoding in *Hermisenda* Photoreceptor Network

Christopher R. Butson and Gregory A. Clark

Department of Biomedical Engineering, University of Utah, Salt Lake City, Utah

Submitted 29 November 2006; accepted in final form 11 November 2007

**Butson CR, Clark GA.** Mechanisms of noise-induced improvement in light-intensity encoding in *Hermisenda* photoreceptor network. *J Neurophysiol* 99: 155–165, 2008. First published November 14, 2007; doi:10.1152/jn.01250.2006. In a companion paper we showed that random channel and synaptic noise improve the ability of a biologically realistic, GENESIS-based computational model of the *Hermisenda* eye to encode light intensity. In this paper we explore mechanisms for noise-induced improvement by examining contextual spike-timing relationships among neurons in the photoreceptor network. In other systems, synaptically connected pairs of spiking cells can develop phase-locked spike-timing relationships at particular, well-defined frequencies. Consequently, domains of stability (DOS) emerge in which an increase in the frequency of inhibitory postsynaptic potentials can paradoxically increase, rather than decrease, the firing rate of the postsynaptic cell. We have extended this analysis to examine DOS as a function of noise amplitude in the exclusively inhibitory *Hermisenda* photoreceptor network. In noise-free simulations, DOS emerge at particular firing frequencies of type B and type A photoreceptors, thus producing a nonmonotonic relationship between their firing rates and light intensity. By contrast, in the noise-added conditions, an increase in noise amplitude leads to an increase in the variance of the interspike interval distribution for a given cell; in turn, this blocks the emergence of phase locking and DOS. These noise-induced changes enable the eye to better perform one of its basic tasks: encoding light intensity. This effect is independent of stochastic resonance, which is often used to describe perithreshold stimuli. The constructive role of noise in biological signal processing has implications both for understanding the dynamics of the nervous system and for the design of neural interface devices.

## INTRODUCTION

Despite considerable progress, the algorithms that biological nervous systems use to process information remain unclear, and the identification of these codes constitutes an area of considerable theoretical and practical interest. Biological systems often outperform their human-engineered counterparts. Identifying the computational strategies used by biological systems to solve complex, ambiguous problems may allow these strategies to be profitably adopted. From a clinical standpoint, understanding neural codes is important for the development of any neural interface or hybrid system, which must necessarily communicate with the nervous system in its own language.

Neural codes can be divided, somewhat artificially, into two classes: 1) population codes, which depend on which neurons are activated (e.g., labeled-line codes), and 2) temporal codes, which depend on how a given population of neurons is acti-

vated (Rieke 1997). A simple temporal code is a rate code, in which increases in neural firing represent increases in a given stimulus parameter. More sophisticated temporal codes depend on the pattern, rather than overall rate, of neural firing. Recently, contextual spike-timing relationships involving firing patterns across groups of neurons have received increased attention. Synchronization of firing represents the best-studied example. Here, information is represented not in the discharge rate or pattern of a single neuron, but in the near-coincident (synchronous) discharge of two or more neurons. Synchrony has been implicated in a variety of sensory and motor processes as well as higher-order cognitive processes such as learning (Fries et al. 1997; Gelperin 2001; Haig et al. 2000; Konig and Engel 1995; Singer 1993; Stopfer et al. 1997; Vaadia et al. 1995), but it has remained difficult to document the causes or consequences of synchrony in a detailed mechanistic way, and its relevance remains controversial, at least to some (Farid and Adelson 2001; Shadlen and Newsome 1994).

Contextual spike-timing codes are distinct both from rate codes and from pattern timing codes that consider only a single neuron's firing in isolation; such codes instead consider the firing rate and/or pattern of a given neuron, relative to the firings of other neurons. As a more specific example, we consider the effects of spike-timing relationships in the *Hermisenda* eye, the details of which are provided in a companion paper (Butson and Clark 2008). Briefly, the *Hermisenda* eye is composed of two type A cells and three type B cells that are connected with exclusively inhibitory synapses. The firing times of type A and type B cells exhibit contextual spike-timing relationships in both the simulated and biological eyes (Fig. 1), which arise in part because of negative feedback connections. Appropriately timed type A cell spikes delay firing of the next type B cell, placing the B spike in a more effective position to inhibit the next A spike. In this way, the relative spike times of pairs of cells can influence the ongoing spike train of the network.

In this paper we use the term “contextual spike timing” to refer to a class of codes, including but not limited to synchrony, that use the relative timing of spikes between or among different neurons. The defining feature of these contextual timing codes is that they rely not only on the rate or pattern of spikes from a given neuron considered in isolation, but rather on the firing of a given neuron in the context of firings of other cells. Central to this research is the observation that contextual spike timing is influenced by ionic and synaptic noise in the *Hermisenda* photoreceptor network. As yet, there is not a detailed understanding of the cellular- or network-level mech-

Address for reprint requests and other correspondence: G. A. Clark, University of Utah, Department of Biomedical Engineering, 20 S. 2030 E., Rm. 506, Salt Lake City, UT 84112-9458 (E-mail: greg.clark@utah.edu).

The costs of publication of this article were defrayed in part by the payment of page charges. The article must therefore be hereby marked “advertisement” in accordance with 18 U.S.C. Section 1734 solely to indicate this fact.

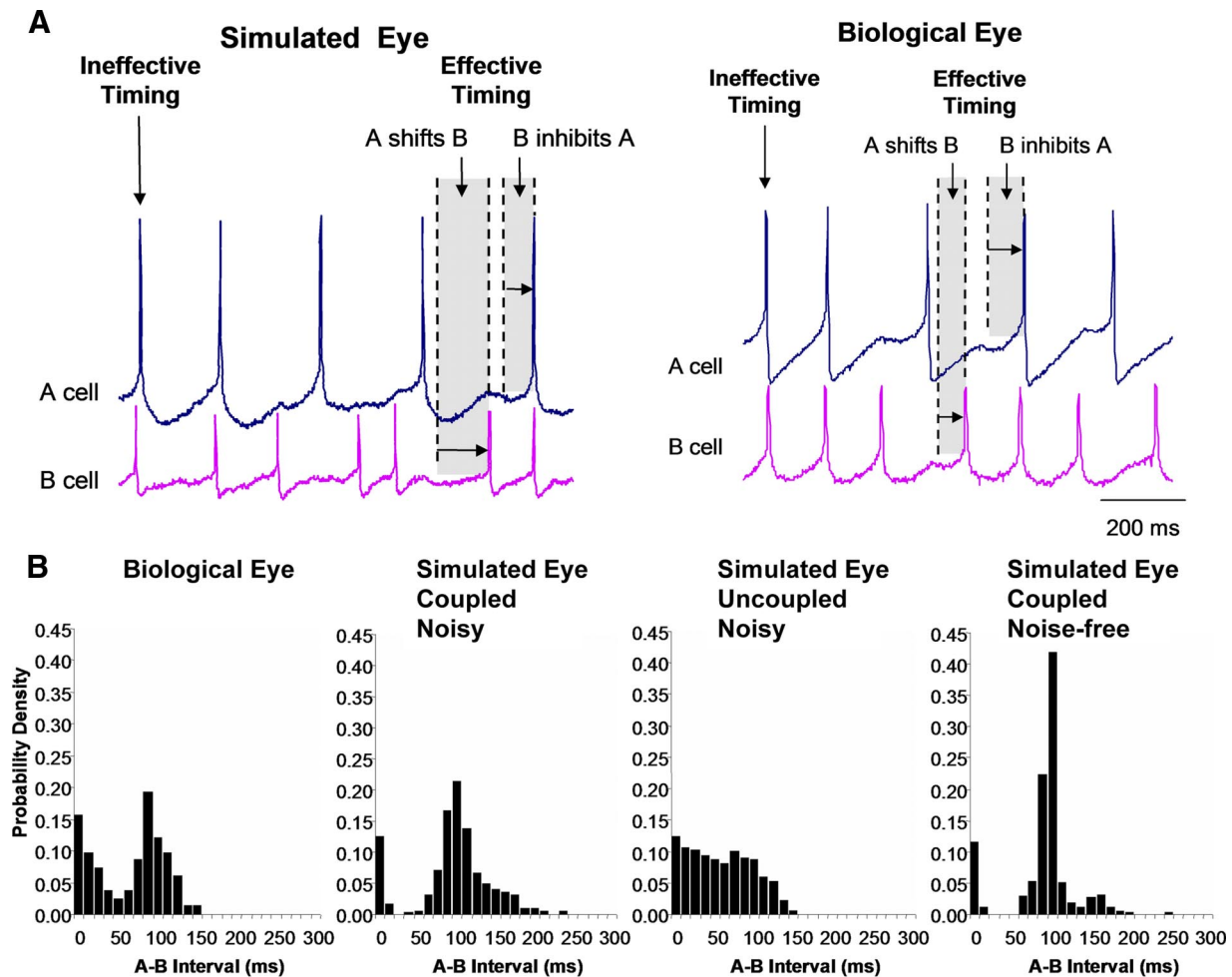


FIG. 1. Contextual spike-timing relationships arise from synaptic connections in the *Hermissenda* eye. *A*: certain relative spike-timing relationships produce little inhibition (“ineffective timing”) between type A cell and type B cell spikes. In contrast, appropriately timed type A cell spikes delay firing of the type B cell, which in turn places the type B spike in a more effective position to inhibit the next type A spike (“effective timing”). These effects occur in both the simulated (*left*) and biological (*right*) eye. As a result, in both the biological eye and the simulated network, there is a striking absence of type B cell spikes shortly after type A cell spikes, as shown by (*B*) the probability distribution of type A cell to type B cell spike-timing intervals. The biological eye (*1st panel from left*) and the simulated noisy eye (*2nd panel*) exhibit similar spike-timing intervals. In the absence of synaptic input (*3rd panel*), no suppression occurs and there are fewer type B cell spikes occurring later in the interval. However, omitting ionic and synaptic noise from the simulated eye alters the shape of the probability distribution but not the time of peak probability (*4th panel*), indicating that noise alters contextual spike-timing relationships.

anisms that generate these codes, although these issues are beginning to be addressed in sensory (Bazhenov et al. 2001a,b), motor (Maex and Schutter 1998), and higher-order (Buzsáki 1997) systems. In the nervous system, time sequences, delays, relatively precise coincidence relationships, and considerations of resolving time seem to be critically important aspects of many information-processing applications (Perkel and Bullock 1968).

In a companion paper we showed that noise paradoxically improves, rather than degrades, the ability of the *Hermissenda* photoreceptor network to accurately encode light intensity (Butson and Clark 2008). In the course of ruling out simple explanations, we discovered intriguing patterns in the firing times of cell pairs; specifically, photoreceptors could become phase locked at certain ranges of light intensities, and this effect was modulated by noise. Could these patterns lead to a mechanistic explanation? In this study, we investigate the mechanisms for noise-induced performance enhancement by exploring contextual spike-timing relationships. We conduct this investigation by examining interactions between noise and

contextual spike-timing relationships in architectures ranging from open-loop cell pairs to the fully connected, five-cell photoreceptor network. Preliminary reports of these results were previously reported (Butson and Clark 2001).

#### METHODS

The purpose of these experiments was to explore mechanisms for noise-induced performance improvement in the *Hermissenda* eye. In a companion paper (Butson and Clark 2008), we provided a detailed description of the computational model used in these experiments. Briefly, we have created a biologically realistic, multicellular, multi-compartment cable model of the *Hermissenda* photoreceptor network based on an earlier model created by Fost and Clark (1996a,b), but with important modifications. First, the model was ported to GENESIS (Beeman and Bower 1998) from a custom C language program. GENESIS is a program with a high-level scripting language that is specifically designed to simulate cable neuron models. This was an important step in providing the model to a larger modeling community and allowing experimental flexibility that otherwise would not have been available. Second, several types of heterogeneity were added

among cells. One attribute of most cable models is that they are deterministic—the computational model yields the same result every time. To explore the effects of randomness in the nervous system, we had to introduce a way to mimic the variation in cell properties that is present physiologically, which we achieved by varying the biophysical properties of each cell in the model eye. Specifically, the membrane resistance of each compartment within each photoreceptor was multiplied by a scaling factor drawn from the Gaussian  $N[1, 0.025]$  distribution. This procedure was repeated to yield 11 model eyes whose results could be compared using parametric statistics. Once selected, these values were fixed for all simulations to mimic heterogeneity in the cell population. In contrast, to investigate effects of noise and the mechanisms of noise-induced improvements in light-intensity encoding, ionic noise was injected into each compartment at each time step through an ionic current drawn from the  $N[0, 0.33 \text{ nA}]$  distribution, and synaptic noise was created by multiplying the quantal force parameter for each spike by a factor drawn from the  $N[1, 0.2]$  distribution. Simulations were performed using a Crank–Nicholson implicit numerical integration scheme with a time step of 0.01 ms. The purpose of these experiments was to examine the performance of the photoreceptor network while encoding light intensity in the presence of noise. Eight light levels were presented to the model eye, representing a change in light intensity of roughly 3.5 log units.

To explore mechanisms for noise-induced performance improvement, we conducted a series of experiments that looked in detail at spike timing between pairs of cells in architectures ranging from open-loop cell pairs to the fully connected network. In open-loop cell pairs, we searched for domains of stability (DOS) in the spike-timing relationships in which the firing of the postsynaptic cell becomes phase locked to the firing of a presynaptic neuron (Perkel et al. 1964). Within such a domain, increases in the firing rate of an inhibitory presynaptic neuron can paradoxically increase the firing rate of its postsynaptic target. In contrast, outside such a domain, increases in inhibition decrease the postsynaptic firing rate as expected. Consequently, monotonic changes in the firing rate of a presynaptic inhibitory input can produce nonmonotonic changes in the firing rate of the postsynaptic target neuron. DOS constitute an emergent property of synaptically connected neurons. Interestingly, DOS can occur with excitatory or inhibitory synapses and do not require feedback connections. In the simplest example from the *Hermisenda* eye, DOS exist at certain combinations of pre- and postsynaptic firing frequencies in a cell pair with a feedforward synapse.

DOS are identified by creating and analyzing delay functions for each type of cell pair (B to A, B to B, A to B), as shown in Fig. 2. In the simplest case of a cell pair with no feedback, the delay function specifies the change in timing of a postsynaptic spike due to a presynaptic spike. They are created by recording pairs of spike times from pre- and postsynaptic cells in the plateau region (last 5 s) of a 10-s light response. The first spike of the postsynaptic cell is fixed at  $t = 0.0$ ; the arrival time of the presynaptic spike is indicated on the abscissa and the resulting delay in the subsequent postsynaptic spike is indicated on the ordinate. In mathematical terms subsequently used here, the delay function specifies the firing delay  $f(\varphi)$  as a function of the inhibitory postsynaptic potential (IPSP) latency  $\varphi$ . The delay functions are analyzed to determine the conditions under which DOS

can occur (see RESULTS), noting that the delay function can be either an analytical function or a curve derived from experimental data (the latter is used herein). We then look for the presence and effects of DOS on different network architectures. Because DOS depends on the relative firing rates of the pre- and postsynaptic neurons, they represent an example of contextual spike-timing relationships. Here we find

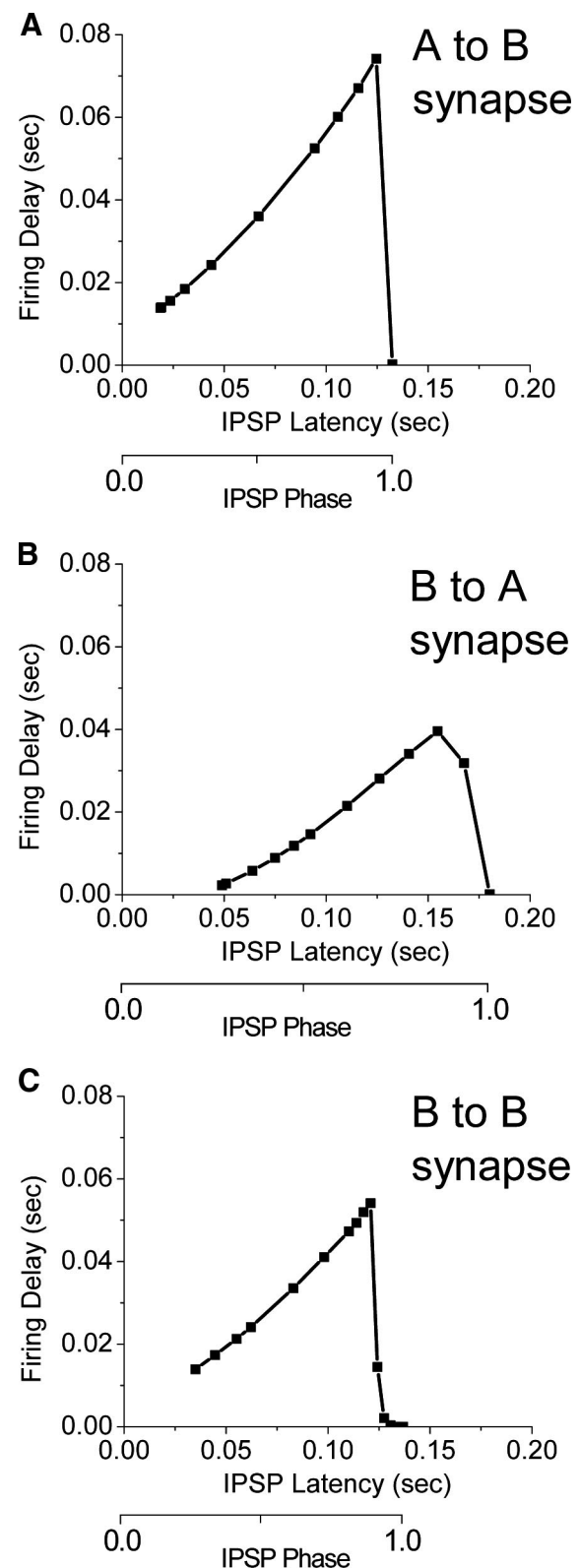


FIG. 2. Delay function curves are shown for (A) type A to type B cells, (B) type B to type A cells, and (C) type B to type B cells. In each curve, a spike in the postsynaptic cell occurs at time  $t = 0.0$ . The inhibitory postsynaptic potential (IPSP) latency (relative to the spike in the postsynaptic neuron) is indicated on the abscissa ( $x$ -axis), and the delay caused by that IPSP on the arrival of the next postsynaptic spike (relative to the time at which the postsynaptic spike would have occurred otherwise) is shown on the ordinate ( $y$ -axis). IPSP arrival is expressed in latency (s) and phase (normalized from 0 to 1, where 1 is the natural period of the postsynaptic cell) as shown on the 2 parallel abscissa scales. The ability of a presynaptic input to change the timing of the next postsynaptic spike depends strongly on where the IPSP falls in the interspike interval (ISI) of the postsynaptic cell.

that the addition of ionic and synaptic noise weakens DOS, and thereby reduces phase locking and the resultant nonmonotonic effects of changes in firing rate of presynaptic neurons. Consequently, photoreceptors respond more accurately to changes in light intensity.

## RESULTS

### *Contextual spike timing is an emergent property resulting from synaptic connections*

Spike times were collected and compiled across many spike pairs. Example intracellular recording traces from the biological and model eye are shown in Fig. 1A, whereas probability distributions for spike firing times for type A to type B cells are shown in Fig. 1B. The biological eye and the simulated noisy eye showed similar A–B spike intervals, indicating that the model accurately represents the firing properties of the system, and that there are emergent spike-timing probability distributions. In the synaptically uncoupled system, this distribution became flat, indicating that the contextual spike timing is an emergent property arising from synaptic interactions, including recurrent negative feedback. Finally, in the noise-free eye, this probability distribution was much more narrow. The sum of these results indicates that contextual spike-timing relationships are an important property of the photoreceptor network and differ between the noisy and noise-free condition, warranting further study.

### *IPSP timing modulates relative firing rate of postsynaptic cells*

Spike-timing relationships in pairs of cells are schematically represented in Fig. 2, which shows delay function curves for IPSPs from presynaptic to postsynaptic cells in an open-loop (no feedback) configuration for A to B, B to A, and B to B cells. In each graph, the postsynaptic cell fires at  $t = 0.0$  and the firing delay of the next spike is indicated as a function of presynaptic IPSP latency. Each delay function curve has two distinct regions. The initial, positively sloping section is the region where IPSPs will delay the firing of the next postsynaptic spike. The final, negatively sloping section results from IPSPs that arrive too late in the interspike interval (ISI) and therefore have little or no effect on the next postsynaptic spike. The delay function has important consequences because if successive IPSPs arrive sooner after  $t = 0.0$  but within the positively sloping region, then the inhibitory input from the presynaptic cell can cause less delay and thus a relative increase in the firing rate of the postsynaptic cell. For example, Fig. 2A shows the delay function for an A cell that is synaptically connected to a B cell. A change in IPSP latency from 0.1 s for the first spike to 0.05 s for the second spike would result in a decrease in the firing delay from 0.057 to 0.028 s, which reflects a relative increase in the firing rate of the B cell. Next we consider what happens if this effect persists in a spike train.

### *IPSP trains can lead to domains of stability even in open-loop cell pairs*

In a continuous spike train, stable patterns can emerge in the firing times of cell pairs even in the absence of feedback. This is best demonstrated when the A and B cells are firing steadily

and spontaneously but at slightly different frequencies, as in response to a light stimulus. Under these circumstances, pairs of synaptically connected cells can exhibit nonmonotonic changes in firing frequency (Fig. 3). In this set of graphs, cell pairs consisting of presynaptic B cells and postsynaptic A cells are stimulated with artificial light currents for 10 s. The stimulus intensity delivered to the postsynaptic A cell is fixed,

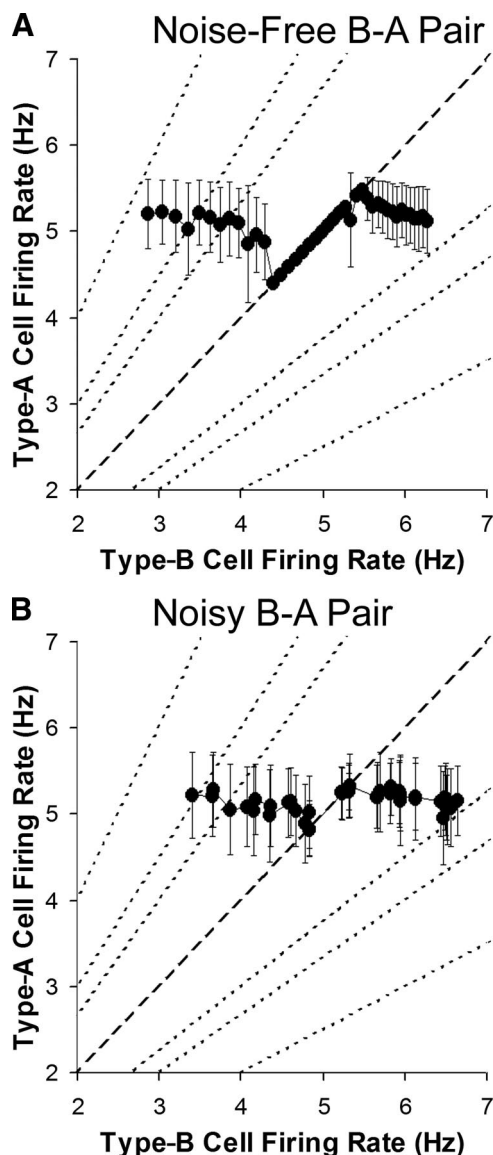


FIG. 3. Domains of stability exist at certain combinations of pre- and postsynaptic firing frequencies. *A*: firing frequencies  $\pm$ SD (calculated on a per-spike basis) in a simulated feedforward B to A cell pair in the noise-free condition exhibit phase locking between roughly 4.5 and 5.5 Hz, shown along the diagonal. Phase locking is reflected in the drastically reduced SD of firing frequency within this domain of stability (DOS). At low firing frequencies ( $<4$  Hz), increases in B cell firing rates slowed A cell firing rates, but as B cell firing rates converged on A cell firing rates, further increases in firing rate of the inhibitory type B cell produce an increase, rather than decrease, in type A cell firing rates. *B*: phase locking is reduced by the addition of noise as reflected in the even distribution of SDs at all firing frequencies, indicating that noise can influence relative spike-timing relationships between type B and type A photoreceptors. Thus, these data illustrate that domains of stability emerge in which an increase in the frequency of inhibitory postsynaptic potentials can paradoxically increase, rather than decrease, the firing rate of the postsynaptic cell. Noise mitigates this effect by interfering with phase locking.

whereas the stimulus to the presynaptic B cell is swept through a range of intensities to produce firing rates that increase from about 3 to 6.5 Hz. The values shown in the graph are the firing frequencies of the cells averaged over the last 5 s of the light step. Because the stimulus to the A cell is fixed but IPSPs are arriving more rapidly as the firing frequency of the B cell increases, one would expect the firing rate of the A cell to decrease as the rate of the B cell inhibitory input increases. However, in the noise-free condition (Fig. 3A), the A cell response becomes strongly nonmonotonic. At relatively low type B cell firing frequencies (<4 Hz), increases in the type B cell spike rate produce modest inhibition of the type A cell firing rate, as expected. As the firing rate of the B cell approaches that of the A cell, however, the A cell rate changes such that it matches the B cell rate in a 1:1 ratio, and the match in firing frequencies is a direct result of phase locking between the two cells, as indicated by the decrease in SD of A cell firing frequency. This ratio persists for a range of presynaptic firing frequencies, first slowing the A cell rate and then speeding up the A cell faster than its original rate. Thus within this DOS, increases in the inhibitory type B cell input can paradoxically increase the type A cell firing rate. Eventually, the A cell can no longer maintain the artificially high firing rate and it drops closer to a value at or below its initial firing rate (leftmost data point in Fig. 3A). Although this effect is most visible at the 1:1 firing rate ratio, these pairs of cells have multiple modes of stable output depending on their relative natural firing frequencies and the strength of the inhibitory connection. DOS can also occur at other integer-multiple frequencies, as will be subsequently shown. Here we have shown that DOS exist and can cause a nonmonotonic relationship between stimulus intensity and firing frequency depending on the rate of inhibitory input.

As we now show more rigorously, DOS can be predicted on the basis of the delay functions shown in Fig. 2. Our approach here is not to find analytical solutions to the governing equations, but rather to derive the equations and show the conditions under which DOS can occur. We begin by examining the phase relationship between pre- and postsynaptic cells at a particular combination of firing frequencies (i.e., for a single data point in Fig. 3). For a cell that is firing in response to light but in the absence of synaptic input, the period of the postsynaptic cell is  $\sigma$ . After the arrival of an IPSP, the period is changed to a new value,  $\sigma'$ , calculated from

$$\sigma' = \sigma + f(\varphi) \quad (1)$$

where  $f(\varphi)$  is the delay function from Fig. 2 that provides the delay of the next postsynaptic spike as a function of the latency  $\varphi$  of the presynaptic IPSP. For a continuous series of pre- and postsynaptic spikes, Eq. 1 can be used with the delay function to predict a train of periods by solving  $\sigma'$  in terms of  $\sigma$ ,  $\sigma'$  in terms of  $\sigma'$ , and so forth. At this point, it is useful to switch from a time-based frame of reference to a phased-based one, as explained in Fig. 4A. That is, instead of predicting the firing times of the cells, we will attempt to predict the latency of each IPSP. As shown in the figure, the latency of the first spike is  $\varphi_i$ , and for constant  $\sigma$  and  $\tau$  values the latency of the second spike is

$$\varphi_{i+1} = \varphi_i + \tau - \sigma - f(\varphi_i) \quad (2)$$

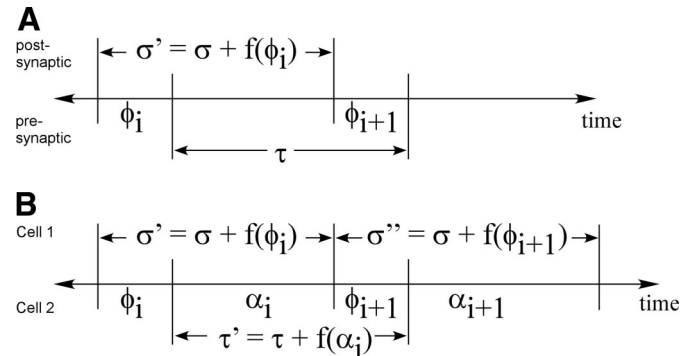


FIG. 4. Spike-timing diagram showing the phase relationship measured between the firing times of the pre- and postsynaptic spikes. Diagram for the open-loop cell pair (A) shows spike times for the presynaptic cell (bottom) and postsynaptic cell (top) as indicated by vertical lines. The firing time of the second postsynaptic spike is determined from the natural period  $\sigma$  of the postsynaptic cell, the phase delay  $\varphi_i$  of the first presynaptic spike, and the delay function  $f(\varphi_i)$ . For the open-loop cell pair,  $\varphi_{i+1}$  is a function of the natural period  $\sigma$  of the postsynaptic cell and the timing of the IPSP, which dictates the firing delay from the delay function. B: in the feedback condition there is an analogous relationship for each cell. In this case the phase relationships for the 2 cells are designated  $\varphi$  and  $\alpha$ , and the two cells are labeled Cell 1 and Cell 2 because the 2 cells are both pre- and postsynaptic (relative to each other).

where  $\tau$  is the stable, limiting value of  $\sigma'$  (in the case of phase locking,  $\tau$  is equal to the constant firing rate of the presynaptic cell). This equation can be used to iteratively predict the latencies of a train of spikes. From this equation it is clear that for some combination of values of  $\sigma$ ,  $\tau$ , and  $f(\varphi)$ , it is possible that

$$\varphi_{i+1} = \varphi_i \quad (3)$$

which would occur if

$$\tau = \sigma + f(\varphi_\infty) \quad (4)$$

where  $\varphi_\infty$  indicates a limiting stable value of  $\varphi$ . Thus under this condition the pre- and postsynaptic cells would be phase locked and firing at the same frequency. Our purpose at this point is to show that it is possible for stable phase relationships to occur such that both cells fire at the same frequency. Next we examine the conditions under which the phase locking is stable over a range of firing frequencies, which would lead to a DOS.

#### DOS have well-defined existence criteria

In the previous section we showed that DOS exist in cell pairs, and that phase locking can occur at particular pre- and postsynaptic firing frequencies. Here we examine the conditions under which these phase-locked relationships are stable. For a train of IPSPs, it is possible to write the phase relationships between cells as

$$\varphi_{i+1} = \varphi_i + f(\varphi_\infty) - [df(\varphi_i)/d\varphi_i] \times \varphi_i \quad (5)$$

where we have substituted Eq. 4 into Eq. 2 and rewritten  $f(\varphi_i)$  as

$$f(\varphi_i) = [df(\varphi_i)/d\varphi_i] \times \varphi_i \quad (6)$$

Equation 5 can be rearranged to yield

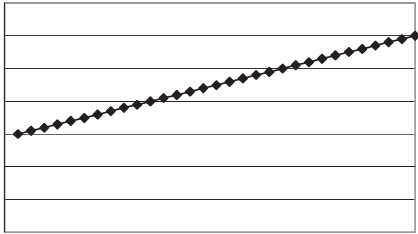
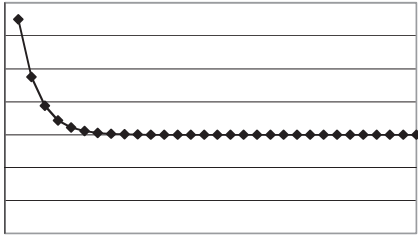
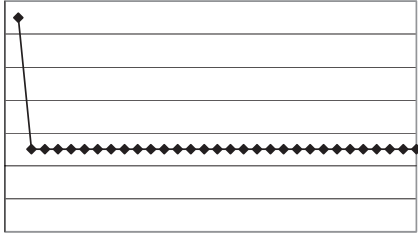
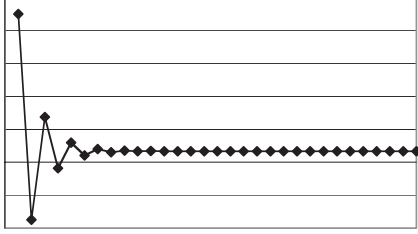
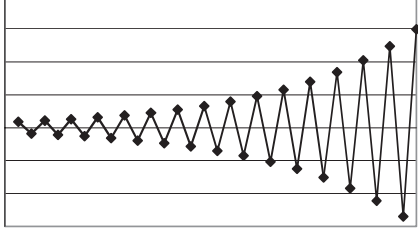
$$\varphi_{i+1} = f(\varphi_\infty) + \varphi_i \times [1 - df(\varphi_i)/d\varphi_i] \quad (7)$$

where the final term in brackets is referred to as the proportionality factor. When viewing the system from the standpoint

of the stable phase value  $f(\varphi_\infty)$ , the proportionality factor can be used to intuit the behavior of the system as described in Table 1. In particular, we can use this equation to determine how the spike latencies change from one spike to the next and therefore how the latencies might evolve to the stable limiting value. Our approach is to assume that a stable phase value  $\varphi_\infty$

exists and that the delay function  $f(\varphi_\infty)$  is well defined at this value [thus  $f(\varphi_\infty)$  is constant in this equation]. Therefore the only values that change from one spike to the next are the latency  $\varphi_i$  and the proportionality factor, which depends on the slope of the delay function  $df(\varphi_i)/d\varphi_i$ . The data shown in Table 1 indicate the qualitative behavior of the system in a

TABLE 1. *Effects of delay function slope on proportionality factor*

| Delay Function Slope               | Proportionality Factor   | Time Evolution of $\varphi$  |
|------------------------------------|--|--|
| $df(\varphi_i)/d\varphi_i = 0$     | Proportionality factor = 1; the magnitude of $\varphi_i$ grows linearly with each iteration. The rate of growth is proportional to $\tau - \sigma$ , which is equivalent to $f(\varphi_\infty)$ as shown in Eq. 4. |    |
| $0 < df(\varphi_i)/d\varphi_i < 1$ | Proportionality factor is between 0 and 1; $\varphi_i$ approaches $\varphi_\infty$ asymptotically.   |   |
| $df(\varphi_i)/d\varphi_i = 1$     | Proportionality factor = 0; $\varphi_i$ reaches $\varphi_\infty$ in one step.  |  |
| $1 < df(\varphi_i)/d\varphi_i < 2$ | Proportionality factor is between 0 and -1; $\varphi_i$ oscillates and magnitude of $(\varphi_i - \varphi_\infty)$ decreases with each iteration.  |  |
| $df(\varphi_i)/d\varphi_i \geq 2$  | Proportionality factor is -1 or less; $\varphi_i$ oscillates and magnitude of $(\varphi_i - \varphi_\infty)$ increases with each iteration.  |  |

For delay function slopes between 0 and 2 (middle 3 rows),  $\varphi_i$  can converge to  $\varphi_\infty$ , as indicated by Eq. 7, and phase locking can occur. Outside of this range,  $\varphi_i$  cannot evolve to  $\varphi_\infty$ .

series of IPSPs, which can be summarized as follows. If the IPSP latency occurs where the slope of the delay function is between 0 and 2, then a stable phase value exists and phase locking can occur; further, if this phase locking persists over a range of firing frequencies, then a DOS will emerge. In contrast, if the slope of the delay function is  $\leq 0$  or  $\geq 2$ , then no stable phase value exists and phase locking cannot occur. This analysis can also be extended to predict the stability of firing frequencies at arbitrary integer ratios. Now that we have shown the existence criteria for DOS in the *Hermisenda* photoreceptor, we will consider the effects of noise.

### Noise modulates DOS

We have shown that DOS occur and that their existence can be inferred from the slope of the delay functions for *Hermisenda* cell pairs. However, the derivation of DOS criteria has assumed constant values for  $\sigma$  and  $\tau$ . A logical question arises: what if a certain amount of jitter exists in the firing times of these cells? More specifically, for cells that maintain average values of  $\sigma$  and  $\tau$ , what is the effect of variance in the length of each ISI period? We found that variance of sufficient magnitude strongly reduces DOS in cell pairs. Figure 3 shows the firing frequencies of an open-loop cell pair consisting of a presynaptic B cell and a postsynaptic A cell. Each data point in the graphs is a unique combination of A and B cell firing frequencies. In all cases, the A cell is stimulated with an artificial light stimulus that does not change between experiments. In contrast, the B cell is subjected to a range of light intensities that increase incrementally with each experiment. In the absence of any synaptic connections, we would expect the average A cell firing to be virtually identical in each experiment, and the average B cell rate to increase monotonically. In the noise-free condition, we observed the firing rate of the A cell changes considerably as a function of average B cell firing rate (Fig. 3A). In contrast, the noisy condition shows little phase locking (Fig. 3B). With the exception of a small collection of points near the 1:1 line, the B cell does not appear to exert much effect on the A cell, aside from a modest inhibition of the type A cell firing rate. Therefore with variable-interval artificial IPSPs, the DOS observed in the noise-free condition is abolished.

Thus DOS are modulated by noise. Specifically, noise smooths the relationship between IPSP input and output firing rates. These results demonstrate that changes in IPSP timing are sufficient to reduce phase locking in the biological eye. Noise improves performance by interfering with phase locking that occurs in DOS. Moreover, this effect cannot be discerned by looking at firing rates alone or by looking at individual spike pairs. The only way to reach this conclusion is by examining contextual spike-timing relationships between pairs of cells. In the noise-free network, light monotonically increases the firing rate of both type A cells and type B cells. B cell input to the A cell has a nonmonotonic effect, producing both expected decreases and anomalous increases in A cell firing (from phase locking within the DOS). The net output of A cells is a nonmonotonic function of light intensity. By contrast, in the noisy network, light monotonically increases firing rate of both type A cells and type B cells. B cell input to type A cells has

a monotonic, inhibitory effect (because the phase locking and anomalous increases are reduced by noise). Thus the net output of A cells is a monotonic function of light intensity.

### Feedback reduces convergence time of DOS

The effect of feedback is incorporated using a modified phase-relation diagram as shown in Fig. 4B. In the feedback condition, the nomenclature of pre- or postsynaptic is somewhat arbitrary because it varies on a per-spike basis. Instead, it is useful to simply rewrite the phase relationships on a per-cell basis. Consistent with the analysis provided earlier, the phase relationships for each successive spike for each cell are given by

CELL 1

$$\varphi_i + \tau' = \sigma' + \varphi_{i+1} \quad (8)$$

$$\varphi_{i+1} = \varphi_i + \tau' - \sigma' \quad (9)$$

$$\varphi_{i+1} = \varphi_i + \tau + f(\alpha_i) - \sigma - f(\varphi_i) \quad (10)$$

CELL 2

$$\alpha_i + \sigma'' = \tau' + \alpha_{i+1} \quad (11)$$

$$\alpha_{i+1} = \alpha_i + \sigma'' - \tau' \quad (12)$$

$$\alpha_{i+1} = \alpha_i + \sigma + f(\varphi_{i+1}) - \tau - f(\alpha_i) \quad (13)$$

At this point it would be useful to express *Eq. 10* in terms of  $\varphi$  and *Eq. 13* in terms of  $\alpha$  [in other words, remove references to  $f(\alpha_i)$  and  $f(\varphi_{i+1})$ , respectively]. To achieve this, two additional relationships are made for each cell. First, from Fig. 4B the following relationships are written for the periods encompassed by  $\sigma'$  and  $\tau'$ , respectively

$$\sigma + f(\varphi_i) = \varphi_i + \alpha_i \quad (14)$$

$$\tau + f(\alpha_i) = \alpha_i + \varphi_{i+1} \quad (15)$$

Second,  $f(\varphi_i)$  and  $f(\alpha_i)$  are rewritten as [also shown in *Eq. 6* for  $f(\varphi_i)$ ]

$$f(\varphi_i) = [df(\varphi_i)/d\varphi_i] \times \varphi_i \quad (16)$$

$$f(\alpha_i) = [df(\alpha_i)/d\alpha_i] \times \alpha_i \quad (17)$$

*Equations 16* and *17* are now substituted into *Eqs. 14* and *15*, respectively, and rearranged to yield

$$\alpha_i = \sigma + \varphi_i \times [df(\varphi_i)/d\varphi_i - 1] \quad (18)$$

$$\varphi_{i+1} = \tau + \alpha_i \times [df(\alpha_i)/d\alpha_i - 1] \quad (19)$$

Now the phase relationships for Cell 1 and Cell 2 can be rewritten. *Equations 16* and *18* are substituted into *Eq. 10* and rearranged to yield

CELL 1

$$\varphi_{i+1} = \tau - \sigma \times [1 - df(\alpha_i)/d\alpha_i] + \varphi_i \times [1 - df(\alpha_i)/d\alpha_i] \times [1 - df(\varphi_i)/d\varphi_i] \quad (20)$$

TABLE 2. Phase equation components expressed in the form of Eq. 22

|                           | f(phase <sub>final</sub> )                                    | Proportionality Factor   |
|---------------------------|---|--|
| Eq. 7 (open-loop)         | $f(\varphi_\infty)$ or $\tau - \sigma$                        | $[1 - df(\varphi_i)/d\varphi_i]$   |
| Eq. 20 (Cell 1, feedback) | $\tau - \sigma \times [1 - df(\alpha_i)/d\alpha_i]$           | $[1 - df(\alpha_i)/d\alpha_i] \times [1 - df(\varphi_i)/d\varphi_i]$         |
| Eq. 21 (Cell 2, feedback) | $\tau - \sigma \times [1 - df(\varphi_{i+1})/d\varphi_{i+1}]$ | $[1 - df(\alpha_i)/d\alpha_i] \times [1 - df(\varphi_{i+1})/d\varphi_{i+1}]$ |

Similarly, Eqs. 17 and 19 are substituted into Eq. 13 and rearranged to yield

CELL 2

$$\alpha_{i+1} = \tau - \sigma \times [1 - df(\varphi_{i+1})/d\varphi_{i+1}] + \alpha_i \times [1 - df(\alpha_i)/d\alpha_i] \times [1 - df(\varphi_{i+1})/d\varphi_{i+1}] \quad (21)$$

It is now possible to compare Eqs. 20 and 21 with Eq. 7 to develop a sense of the phase behavior. Specifically, all three of these equations can be expressed in the form

$$\text{phase}_{i+1} = f(\text{phase}_{\text{final}}) + \text{phase}_i \times \text{proportionality factor} \quad (22)$$

and the different components of the equations are summarized in this form in Table 2.

To understand why feedback speeds convergence, it is necessary to take note of two things. First, the closer the proportionality factor is to 0, the faster the phase will converge. Second, the magnitude of the proportionality factor is decreased in the feedback condition relative to the open-loop condition. To see why this is the case, let us make the simplifying assumption that

$$df(\varphi)/d\varphi = df(\alpha)/d\alpha = \text{constant in the range } (0, 2) \quad (23)$$

Then, using the information provided in Table 2, the proportionality factor for the open-loop condition is  $[1 - df(\varphi)/d\varphi]$ , whereas the proportionality factor for the feedback condition is  $[1 - df(\varphi)/d\varphi]^2$ . Because  $df(\varphi)/d\varphi$  is in the stable range (0, 2),  $[1 - df(\varphi)/d\varphi]$  is in the range (-1, 1), and the magnitude of the proportionality factor for the feedback condition is smaller than that for the open-loop condition. Therefore the feedback condition converges faster. The stability of the phase relationship for the feedback condition is qualitatively unchanged from Table 1, given that the proportionality factor is now calculated using the expressions in Table 2 that incorporate the delay function slopes for Cell 1 and Cell 2.

The effects of feedback can be observed in cell pairs by examining changes in ISI as a function of time. In this analysis the stable ISI was found by running simulations with open-loop and feedback connections in the noise-free condition until the cells converged on a stable phase relationship (10 s was sufficient). Light intensities were chosen such that the mean firing rate in the open-loop and feedback conditions were within 0.05 Hz of each other at the end of the trial. Then, the magnitude difference in ISI between each successive spike pair and the final spike pair was determined and plotted as a function of time, as shown in Fig. 5. These results confirm what we expect from the theoretical analysis: the presence of feedback reduces convergence time of the DOS relative to the open-loop condition.

### Noise improves performance by abolishing DOS

In the fully connected network, noise improves performance by interfering with phase locking that occurs within DOS. Figure 6 shows the effects of noise in the fully connected network. In the noise-free condition, phase locking induces a paradoxical increase in type A cell firing rate as A cell and B cell firing rates converge, disrupting light intensity encoding. In the noisy condition, the anomalous increases in type A cell firing are ameliorated by noise. Thus noise alters contextual spike-timing relationships and reduces phase locking. As a result, the performance of the eye in encoding light intensity is improved, enabling the animal to make faster and more accurate measurements of its surrounding environment.

### DISCUSSION

This paper has presented a sequence of experiments that demonstrate how random noise and its effects on contextual spike timing can lead to improved performance of the *Hermisenda* photoreceptor network. The key mechanistic feature of the enhanced performance involves contextual spike timing, which is an emergent network property that may help explain how networks of neurons are smarter than individual cells. These results are pertinent because they elucidate an example of contextual spike timing, how it is distinct from rate codes or population codes, and how this type of code cannot be inferred from individual cells in isolation. We have shown that these codes can arise in isolated cell pairs with no feedback and that they persist in larger cell networks with feedback connections. This effect is highlighted by the data shown in Fig. 7. There are two opposing effects of type A cell firing frequency in the *Hermisenda* eye: light-induced depolarization increases

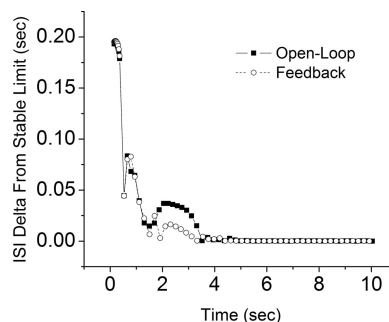


FIG. 5. Synaptic feedback speeds convergence time. The plot shows changes in duration of ISI over time as it evolves to the stable limit. Specifically, the magnitude difference in ISI between each successive spike pair and the final spike pair (which represented the stable limit) is plotted as a function of time during a 10-s light stimulus. Data are shown for both open-loop and feedback synaptic connections in the noise-free condition. Feedback connections speed convergence time and improve the accuracy of the network. The nonmonotonicity of the phase evolution in the early part of the curve is caused by individual cell adaptation to the light response.

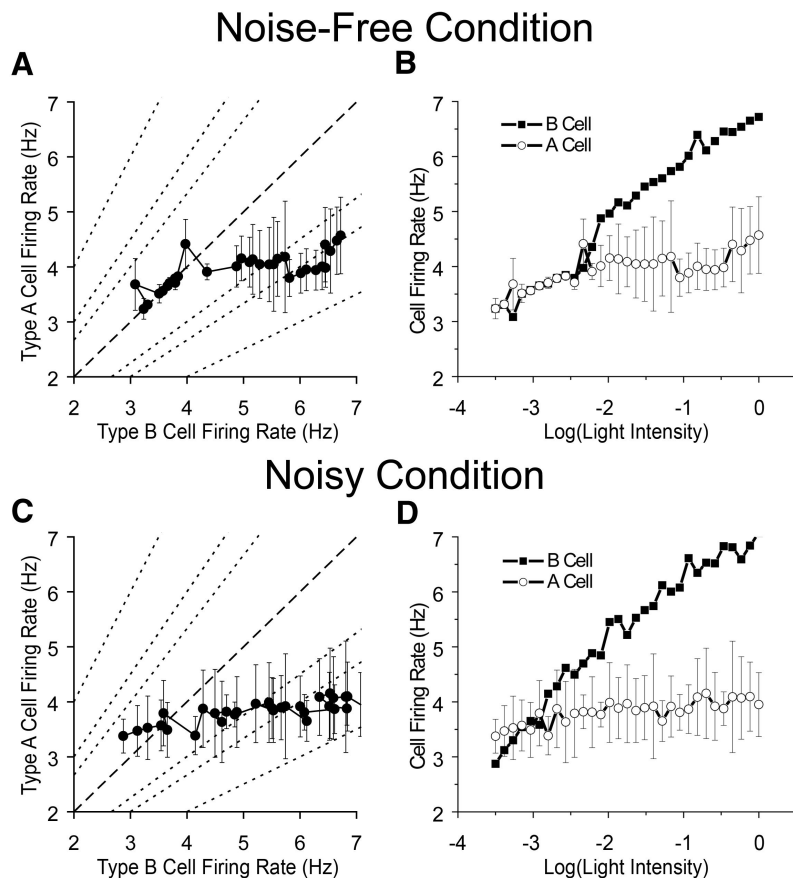


FIG. 6. Noise improves light-intensity encoding by reducing phase locking. The effects of phase locking are preserved in the fully connected network, as shown by the correspondence between the firing rates of type A and type B cells collected over a range of light intensities. *A* and *B*: noise-free networks. Similar to Fig. 3, *A* shows the relationship between frequencies of one type A and one type B cell with the DOS visible along the 1:1 ratio (dashed line). To better illustrate this, *B* shows free-running firing rates of both cells in response to a range of light intensities, with the firing rates of the 2 cells matched at several points for lower light intensities. Data show the average type A cell frequency  $\pm$ SD; SDs of type B cells are similar but omitted for clarity. Thus, there is a paradoxical increase in type A cell firing rate, despite the increased inhibition from type B cells, caused by phase locking within this DOS. A lesser degree of phase locking may also occur at other fractional ratios of firing rates (4:3 and 3:2, short-dashed lines). *C* and *D*: in noisy networks, there is little apparent phase locking, and the anomalous increase in type A cell firing rate within the DOS is greatly diminished. Phase locking in type B cells is also reduced at low light levels, resulting in a roughly monotonic relationship between firing rate and light intensity.

the firing frequency (A cell light only); inhibitory input from type B cells (B cell light only) decreases type A cell firing frequency, particularly in the absence of phase locking (A cell synaptic input only). Thus, in the absence of phase locking, the type A cell rate is expected to be intermediate between light alone and inhibitory input alone (A cell expected). In contrast, in the presence of phase locking, the type A cell firing rate changes nonmonotonically as a function of light intensity, both in B-to-A cell pairs (A cell with B input) and in the fully connected network (A cell with network input). Thus phase locking degrades light-encoding performance.

Similar ideas have also been proposed in simple model systems. “Noise shaping” has been shown as an important phenomenon in a network of coupled integrate-and-fire model neurons (Mar et al. 1999). Noise shaping allows the population to encode signals over a wide bandwidth and improved signal-to-noise ratio. The mechanism for this improvement comes about because noise and heterogeneity in the network help serve to break up clustering and stabilize the asynchronous firing rate and may also boost weak signals above threshold. However, when the neurons are coupled by inhibition, both signal and noise power are reduced from their values in the uncoupled network. Thus the coupling disfavors short ISIs in the network and spaces out firing events. It has also been shown that deterministic Hodgkin–Huxley neurons can exhibit entrainment to rhythmic stimuli in the absence of noise (Read and Siegel 1996). Only heterogeneity in synaptic delays was necessary to produce this effect in a network of neurons. They reported

that simply driving a model or real neuron with a random input is not a sufficient way to generate highly variable spike trains. Additional sources of “jitter” for entrainment of sensory neurons could be inherent membrane properties, synaptic potential kinetics, or axonal conductance delays. Finally, probabilistic—rather than deterministic—ion channels increase the cell’s repertoire of qualitative behavior (White et al. 1998).

Many investigators have provided evidence of coding schemes beyond rate or population codes. Preliminary support for the existence and importance of contextual spike timing was provided by Segundo et al. (1963), who made several observations in the visceral ganglion of *Aplysia californica*. First, the higher-order statistics of spike arrival times have an important effect on physiological response, even when controlling for mean firing frequency. They asserted that sensitivity to timing could be biologically advantageous, especially in areas of sensory convergence, because it provides an additional coding parameter complementing mean frequency modulation. However, frequency is not an adequate specification or a candidate code—it is really a class of codes. The information relevant to the decoder may be represented by the value of the most recent ISI, or averaged over some period. In fact, over a dozen codes have been identified based on rate alone (Perkel and Bullock 1968). More recently, neurons in a sensory system have been shown to respond very differently to spike trains with comparable mean firing rates but different statistics (Bialek and Rieke 1992). Although here we use the term “contextual spike timing” to refer to temporal relationships, Tiesinga and Jose

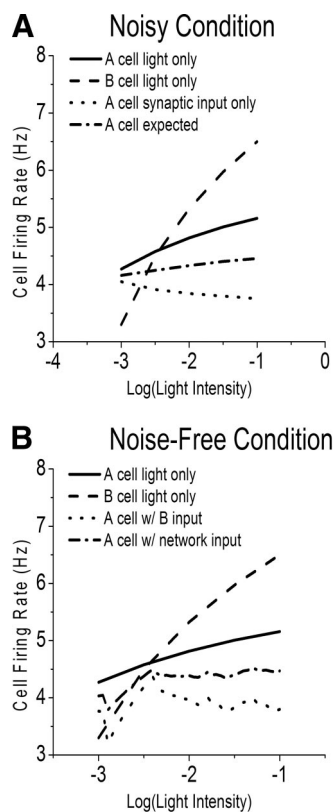


FIG. 7. DOS in the fully connected network. *A*: there are 2 opposing effects of type A cell firing frequency in the *Hermisenda* eye: depolarization due to light increases the firing frequency (A cell light only); inhibitory input from type B cells (B cell light only) decreases type A cell firing frequency (A cell synaptic input only). In the absence of phase locking, the type A cell rate is expected to be intermediate between light alone and inhibitory input alone (A cell expected). *B*: in the presence of phase locking, type A cell rate changes nonmonotonically as a function of light intensity, both in B to A cell pairs (A cell w/B input) and in the fully connected network (A cell w/network input). Thus phase locking degrades light encoding performance.

(2000) make a distinction between strong and weak synchronization. The former requires that spikes occur within a specific time window of each other, whereas the latter is more general. In weak synchronization, the average neuronal activity is periodic, without each individual neuron having to fire at each period. Their experiments on a Hodgkin–Huxley network model of thalamic neurons suggest that weak synchronization is robust against neuronal heterogeneities and synaptic noise, and that it can encode more information compared with strongly synchronized states. They also found that noise amplitudes play an important effect in synchronization: for small networks, more noise is required to drive the subthreshold network into stable oscillations.

Stochastic resonance (SR) is a simple mechanism that has often been used to explain the dynamics of neural systems in the presence of noise. For example, Longtin et al. (1994) showed conditions under which periodically stimulated neurons can be modeled as bistable systems embedded in noise. More important, they showed that the dynamics of this simple system, which mimic those of ISI histograms from cat and monkey, cannot exist in the absence of noise (Longtin et al. 1991). The dynamics of noise can also play a critical role in signal processing. Noise sources that are identical, independent, or spatially correlated have been shown to have important differences for stochastic resonance in a network of Hodgkin–

Huxley neurons (Liu et al. 2001). Added internal neuronal noise can improve the timing precision of deterministically subthreshold stimuli, and optimal noise results in maximal improvement (Pei et al. 1996). By contrast, noise degrades only the timing precision of suprathreshold stimuli. More specific to sensory systems, Collins et al. (1996) examined SR in rat slowly adapting type 1 afferents with aperiodic inputs. They found clear SR behavior in 11 of 12 neurons tested. In contrast, the phenomenon we report here is independent of SR for two reasons. First, SR is normally associated with perithreshold stimuli, whereas the stimuli used in these experiments are all suprathreshold. Second, the results from SR experiments are well explained by use of a bistable system, where noise facilitates transitions from one state to another. Clearly, the spike-timing dynamics in the *Hermisenda* photoreceptor cannot be explained by either of these scenarios.

Other mechanisms for the apparent noisiness in neurons have also been proposed. Liebovitch and Toth (1991) conducted a series of experiments to show that ion channel kinetics can be represented by deterministic chaos rather than a stochastic process. With this representation, the ion channel model is an iterated map that is piecewise linear. Clay and Shrier (1999) used a Fitzhugh–Nagumo model to show that randomness in ISI can be attributable to deterministic chaos rather than to a stochastic noise source. In our analysis we avoided the use of chaos as a mechanism for two reasons. First, although chaotic behavior can certainly emerge from a system governed by dynamic differential equations, the criteria for the ongoing presence of chaos in such a system are not easily established. Second, and more important, the use of chaos is unnecessary to explain the observed dynamics of the system.

The constructive effects of noise in sensory signal processing has implications for our understanding of neural dynamics, as well as the design of neural interface devices. From the perspective of basic science, the existence of contextual spike-timing codes is an addition to our understanding of the way the nervous system communicates. Contextual spike-timing codes have previously been proposed, such as synchrony in mammalian visual cortex as a potential solution to the “binding” problem. However, it has been difficult to document their importance empirically. The relatively simple neural circuit of the *Hermisenda* eye has allowed a detailed analysis of both the role of contextual spike timing codes and the mechanisms that underlie their emergence. The existence of this type of code in *Hermisenda* demonstrates that neural communication depends on well-spaced neural spike times and that it is necessary to measure the relative spike times of multiple neurons to understand this code. The effects of noise as demonstrated herein and in the companion paper are based on an inhibitory-only network. However, the phenomenon is not limited to inhibitory networks. Recent results have shown it to be equally prevalent in excitatory networks (Clark and Legge 2006); it is also hypothesized to occur in mixed excitatory/inhibitory networks. Preliminary results have been reported for the former (Perkel et al. 1964) and the implications of the latter could be significant for understanding cortical dynamics. This is particularly interesting in the context of diseases with pathological synchronization such as Parkinson’s disease and epilepsy, which might be treated by artificially increasing noise levels.

## ACKNOWLEDGMENTS

We thank C. Johnson, G. Jones, J. Wiskin, R. Normann, and D. Beeman for comments on an earlier version of this manuscript.

## GRANTS

This work was supported by the Whitaker Foundation and National Institute of Mental Health Grant R01-MH-068392.

## REFERENCES

- Bazhenov M, Stopfer M, Rabinovich M, Abarbanel HD, Sejnowski TJ, Laurent G.** Model of cellular and network mechanisms for odor-evoked temporal patterning in the locust antennal lobe. *Neuron* 30: 569–581, 2001a.
- Bazhenov M, Stopfer M, Rabinovich M, Huerta R, Abarbanel HD, Sejnowski TJ, Laurent G.** Model of transient oscillatory synchronization in the locust antennal lobe. *Neuron* 30: 553–567, 2001b.
- Bialek W, Rieke F.** Reliability and information transmission in spiking neurons. *Trends Neurosci* 15: 428–434, 1992.
- Bower JM, Beeman D.** *The Book of GENESIS: Exploring Realistic Neural Models with the GEneral NEural Simulation System* (2nd ed.). New York: Springer-Verlag, 1998.
- Butson CR, Clark GA.** Random noise confers a paradoxical improvement in the ability of a simulated *Hermisenda* photoreceptor network to encode light intensity. *Soc Neurosci Abstr* 954.6, 2001.
- Butson CR, Clark GA.** Random noise paradoxically improves light-intensity encoding in *Hermisenda* photoreceptor network. *J Neurophysiol* (January 2008). doi:10.1152/jn.01247.2008.
- Buzsáki G.** Functions for interneuronal nets in the hippocampus. *Can J Physiol Pharmacol* 75: 508–515, 1997.
- Chialvo DR, Guillermo AC, Marcelo OM.** Noise-induced memory in extended excitable systems. *Phys Rev E Stat Nonlin Soft Matter Phys* 61: 5654–5657, 2000.
- Clark GA, Legge M.** Noise enhances information processing in excitatory neural circuits by altering contextual spike-timing relationships. *Soc Neurosci Abstr* 351.8, 2006.
- Clay JR, Shrier A.** On the role of subthreshold dynamics in neuronal signaling. *J Theor Biol* 197: 207–216, 1999.
- Collins JJ, Imhoff TT, Grigg P.** Noise-enhanced information transmission in rat SA1 cutaneous mechanoreceptors via aperiodic stochastic resonance. *J Neurophysiol* 76: 642–645, 1996.
- Farid H, Adelson EH.** Synchrony does not promote grouping in temporally structured displays. *Nat Neurosci* 4: 875–876, 2001.
- Fost JW, Clark GA.** Modeling *Hermisenda*: I. Differential contributions of  $I_A$  and  $I_C$  to type-B cell plasticity. *J Comput Neurosci* 3: 137–153, 1996a.
- Fost JW, Clark GA.** Modeling *Hermisenda*: II. Effects of variations in type-B cell excitability, synaptic strength, and network architecture. *J Comput Neurosci* 3: 155–172, 1996b.
- Fries P, Roelfsema PR, Engel AK, König P, Singer W.** Synchronization of oscillatory responses in visual cortex correlates with perception in interocular rivalry. *Proc Natl Acad Sci USA* 94: 12699–12704, 1997.
- Gelperin A.** Smelling well with a code in the nodes. *Neuron* 30: 307–309, 2001.
- Haig AR, Gordon E, Wright JJ, Meares RA, Bahramali H.** Synchronous cortical gamma-band activity in task-relevant cognition. *Neuroreport* 11: 669–675, 2000.
- Kohn AF, Freitas da Rocha A, Segundo JP.** Presynaptic irregularity and pacemaker inhibition. *Biol Cybern* 41: 5–18, 1981.
- König P, Engel AK.** Correlated firing in sensory-motor systems. *Curr Opin Neurobiol* 5: 511–519, 1995.
- Liebovitch LS, Toth TI.** A model of ion channel kinetics using deterministic chaos rather than stochastic processes. *J Theor Biol* 148: 243–267, 1991.
- Liu F, Hu B, Wang W.** Effects of correlated and independent noise on signal processing in neuronal systems. *Phys Rev E Stat Nonlin Soft Matter Phys* 63: 031907, 2001.
- Longtin A, Bulsara A, Moss F.** Time-interval sequences of bistable systems and the noise-induced transmission of information by sensory neurons. *Phys Rev Lett* 67: 656–659, 1991.
- Longtin A, Bulsara A, Pierson D, Moss F.** Bistability and the dynamics of periodically forced sensory neurons. *Biol Cybern* 70: 569–578, 1994.
- Maex R, Schutter ED.** Synchronization of Golgi and granule cell firing in a detailed network model of the cerebellar granule cell layer. *J Neurophysiol* 80: 2521–2537, 1998.
- Mar DJ, Chow CC, Gerstner W, Adams RW, Collins JJ.** Noise shaping in populations of coupled model neurons. *Proc Natl Acad Sci USA* 96: 10450–10455, 1999.
- Omurtag A, Knight BW, Sirovich L.** On the simulation of large populations of neurons. *J Comput Neurosci* 8: 51–63, 2000.
- Pei X, Wilkens L, Moss F.** Noise-mediated spike timing precision from aperiodic stimuli in an array of Hodgkin–Huxley type neurons. *Phys Rev Lett* 77: 4679–4682, 1996.
- Perkel DH, Bullock TH.** Neural coding. *Neurosci Res Program Bull* 6: 221–343, 1968.
- Perkel DH, Schulman JH, Bullock TH, Moore GP, Segundo JP.** Pacemaker neurons: effects of regularly spaced synaptic input. *Science* 145: 61–63, 1964.
- Read HL, Siegel RM.** The origins of aperiodicities in sensory neuron entrainment. *Neuroscience* 75: 301–314, 1996.
- Rieke F.** *Spikes: Exploring the Neural Code*. Cambridge, MA: MIT Press, 1997.
- Roddey JC, Girish B, Miller JP.** Assessing the performance of neural encoding models in the presence of noise. *J Comput Neurosci* 8: 95–112, 2000.
- Schneidman E, Freedman B, Segev I.** Ion channel stochasticity may be critical in determining the reliability and precision of spike timing. *Neural Comput* 10: 1679–1703, 1998.
- Segundo JP, Moore GP, Stensaas LJ, Bullock TH.** Sensitivity of neurones in *Aplysia* to temporal patterns of arriving impulses. *J Exp Biol* 40: 643–667, 1963.
- Shadlen MN, Newsome WT.** Noise, neural codes and cortical organization. *Curr Opin Neurobiol* 4: 569–579, 1994.
- Singer W.** Synchronization of cortical activity and its putative role in information processing and learning. *Annu Rev Physiol* 55: 349–374, 1993.
- Stopfer M, Bhagavan S, Smith BH, Laurent G.** Impaired odour discrimination on desynchronization of odour-encoding neural assemblies. *Nature* 390: 70–74, 1997.
- Tiesinga PH, Jose JV.** Synchronous clusters in a noisy inhibitory network. *J Comput Neurosci* 9: 49–65, 2000.
- Vaadia E, Haalman I, Abeles M, Bergman H, Prut Y, Slovin H, Aertsen A.** Dynamics of neuronal interactions in monkey cortex in relation to behavioural events. *Nature* 373: 515–518, 1995.
- White JA, Klink R, Alonso A, Kay AR.** Noise from voltage-gated ion channels may influence neuronal dynamics in the entorhinal cortex. *J Neurophysiol* 80: 262–269, 1998.